



UNIVERSITÀ DEGLI STUDI  
DI GENOVA



# In vitro 3D co-culture of mesenchymal stromal cells and Hodgkin Lymphoma cells on Collagen Scaffolds

XXXIII PhD program in Biotechnologies in Translational Medicine

Curriculum: Regenerative Medicine and Tissue Engineering

Phd Student: Roberta PECE

Tutor: Dr. Sara TAVELLA

Co-Tutor: Dr. Maria Raffaella Zocchi

Coordinator: Prof. Rodolfo Quarto

## INDEX

Introduction .....	2
Hodgkin Lymphoma.....	2
Immune response and evasion mechanisms of HL .....	2
Mesenchymal Stromal Cell and HL cells interaction.....	4
Metalloproteases in cancer: the double blade of ADAMs.....	5
Therapeutic treatment for Hodgkin’s lymphoma .....	6
Cell culture model: from <i>in vitro</i> 2D to 3D co-culture systems .....	8
Scope of thesis.....	9
Materials and Methods .....	10
Cell Cultures.....	10
Adam 10 inhibitors.....	10
Spheroid generation and culture.....	10
De-cellularized matrix lymph node preparation.....	11
3D co-cultures on LN de-cellularized matrix.....	11
3D co-cultures on collagen scaffold.....	11
Images and measurement of spheroid size .....	12
Scanning Electron Microscopy of de-cellularized LN matrix and collagen scaffolds .....	13
ATP content in spheroid co-cultures .....	13
Glucose Assay in co-culture medium.....	13
TNF $\alpha$ and sCD30 ELISA .....	14
Hematoxylin-Eosin staining .....	14
Immunohistochemistry (IHC) and Immunofluorescence (IF).....	14
Scanning and computerized imaging.....	15
Results and Discussions .....	16
ADAM10 inhibitors LT4 and MN8 activity on spheroid co-cultures.....	16
ADAM10 inhibitors LT4 and MN8 reduce CD30 and TNF $\alpha$ secretion by HL cells on de-cellularized lymph node matrix and 3D scaffold .....	16
LT4 and MN8 inhibit HL cell proliferation in the 3D repopulated scaffolds .....	20
Sequential seeding and Ki67 IF do not meet our needs: mix seeding and caspase-3 IHC evaluation ..	22
Caspase-3 activation in HL cells upon Bre-Ved and ADAM10 inhibitors treatment .....	24
Conclusions .....	25
Bibliography.....	28

## Introduction

### Hodgkin Lymphoma

Lymphomas originate from the malignant transformation of lymphocytes and are common haematological malignancies in the Western world. The first lymphoma to be recognized was Hodgkin's lymphoma (HL), described by Thomas Hodgkin in 1832; all other lymphomas are known as non-Hodgkin lymphomas (NHL). HL has a bimodal incidence curve, occurring most frequently in young age (between 15-35 years) and in patients over 55 years. Epstein Barr virus (EBV) positive cases are found especially in patients below 10 years of age and older than 60 (1).

HL is characterized by the presence of large mono- or multinucleated Hodgkin cells and binucleated Reed-Stenberg (RS) cells that constitute usually only about 1% of the total cell in the tumour mass. Although RS cells derive from B cells, they lose most of their B cell phenotype: they lack expression of BCR, while CD40-CD40L, Epstein Barr virus-derived latent membrane protein (LMP1) and CD30 are expressed (2). In particular, CD30 is expressed at higher levels by HL/RS cells and a soluble form has been found in the serum of several HL patients (3). The soluble form of CD30 (sCD30) is generated by proteolytic cleavage of metalloproteinase calls ADAMs. It has been shown that ADAM10 is expressed in both HL lymph nodes and HL/RS cells, (4) promoting an immunosuppressive microenvironment.

HRS cells show numerical and structural aberrations. In addition to the common gains and losses of specific chromosomal regions, a chromosomal translocation is recurrent, involving the major histocompatibility class II (MHC II) trans-activator gene locus that has been observed in several cases of HL. It should be noted that MHC peptide  $\alpha$  and  $\beta$  are cleaved by metalloproteinases like CD30 as well. These soluble forms are present in the serum of cancer patients and their levels correlate with tumour stage and metastasis contributing also to tumour cell escape from natural killer (NK) cell-mediated immunosurveillance (5).

### Immune response and evasion mechanisms of HL

The body defends itself against virus, bacteria and foreign substances through immune responses. We can identify two different immune response pathways: innate and adaptive response. The innate immune response works through the activation of myeloid cells, such as macrophages, and soluble factors including cytokines and complement, it is rapid and non-specific; the adaptive branch is the body's immune response against specific antigens and for this reason it takes longer

to activate all the components involved. The antigen specific immune response includes antigen-presenting cells (APC), T and B cells, antibodies and all the adaptive responses which require several steps. Evading immune system is a prerequisite for neoplastic progression and this ability is linked to the expression of several stress-induced molecules that are known as natural killer receptor group 2 ligands (NKG2DL). In non-pathological conditions NKG2L stimulate NKG2D on the surface of natural killer cells (NK) or gamma delta T cells ( $\gamma\delta$ -T) (4). The interaction between NKG2D-NKG2DL results in the release of granzyme and perforin and antitumor cytokines like tumour necrosis factor  $\alpha$  (TNF $\alpha$ ) to trigger antitumor immune response. Tumors, including lymphomas, may become invisible through several mechanisms. Raneros and co-workers (6) highlight how stress molecules such as MICA and MICB can be cleaved in malignant cells by protein metalloproteases ADAM10 and protein disulphide isomerase family A, also known as ERp5 (7) and be released as soluble molecules; soluble NKG2DL thus masks NKG2D and the signal cannot be activated.

In addition, HL/RS cells can be found in the presence of non-malignant inflammatory, mesenchymal cells, T and B lymphocytes, eosinophils, neutrophils and plasma cells, unable to induce an effective anti-tumour immune response and providing survival signals by secretion of cytokines and chemokines (8) (9). It has been described that HL mesenchymal stromal cells (MSC) express very low levels of MICA and MICB, while high expression of metalloproteases and isomerases, in particular ADAM10 and ERp5, is observed. Since ADAM10 and ERp5 are both correlated with the shedding of stress molecules, including NKG2DL, we can hypothesize that microenvironment and cell interaction in HL play an important role in determining an anti-tumor immune response (4). In addition, genetic modifications cooperate with microenvironment signalling in the activation of pro-tumoral pathways like Nuclear Factor-Kappa $\beta$  (NF-K $\beta$ ) and JACK-STAT. Different mechanism can be described related with NF-K $\beta$  pathways. For instance, Epstein-Barr virus (EBV) is consistently associated with HL in 40% of cases (10). EBV virus Latent Membrane Protein 1 (LMP1), a member of tumor necrosis factor receptor (TNFR), is involved in NF-K $\beta$  activation leading to an overexpression of antiapoptotic molecules and inflammatory cytokines (11). As well as LMP1 another member of TNFR is CD30 that is consistently detected on HL/RS cells. Since 1989 ELISA assay revealed that sCD30 is present at a very low levels in serum obtained from healthy donors, while increasing serum sCD30 has been observed in several conditions including HL (12) (13). Stimulation of CD30 with its ligand CD30L can induces pleiotropic effects including proliferation and cytokine secretion (14). Mir et al. suggested that a constitutive activation of NF-K $\beta$  signalling in HL cell lines could lead to impaired sensitivity to CD30-mediated pro-apoptotic signalling (15). CD30 is another substrate

of ADAM10 protease, its extracellular domain can be cleaved and a soluble form (sCD30) is released. In particular, shedding of CD30 blocks the interaction between specific antibodies anti-CD30 like Brentuximab-Vedotin, giving a further advantage to the tumor cells (16) (17). A recently identified mechanism of immune evasion is the inhibitory molecule programmed death-1 (PD-1) and its ligand PD-L (18). In HL, PD-L is overexpressed both by malignant and surrounding cells and in thus depress the adaptive immune system in a process called “T-cell exhaustion”. In addition, PD-L is overexpressed by LMP1, which mimics CD40 signalling, and this highlight how these mechanisms are correlated to each other.

Macrophages are another class of cells abundant in HL microenvironment. Indeed, exposure to soluble factors such as IL-4 and 13, produced by HL cells, leads to polarization of macrophages to the M2 phenotype, which suppresses cytotoxic T cell activity, facilitating tumor immune escape (19).

#### Mesenchymal Stromal Cell and HL cells interaction

All the cells described above reside in a complex microenvironment where interactions occur with the extracellular matrix (ECM), mainly composed by collagen, fibronectin, and laminin. Here MSC play a key role defining tissue architecture and monitoring tissue homeostasis. In addition, MSC secreted trophic factors are capable to promote tissue repair and immune modulation. MSC are responsible for the production of both components of ECM and enzymes that can modify ECM structure. For example, healthy fibroblast express low levels of activation protein (FAP) but expression increases during wound healing, osteoarthritis and in other pathological conditions (20). However, FAP is expressed by several tumor cells and thus it is difficult to distinguish the contribution of MSC from that of tumor cells. It is well known that there is not a single specific marker to identify MSC, but transglutaminase II (TGII) can be used to mark MSC by immunohistochemistry and cytofluorimetry (21). TGII is involved in many biological processes in cancer, such as tumor cell proliferation and apoptosis (22).

Previous reports have found that MSC can alter the function of immune cells with both cell-to-cell contact and the secretion of soluble cytokines. MSC express some counter-ligands for lymphocyte receptors involved in lymphocyte-MS interaction (23) (19). In particular, the response of B cells to MSC is closely associated to the microenvironment. When MSC are co-cultured with B cells in 2D *in vitro* conditions, they regulate immunoglobulin secretion, apoptosis, proliferation, plasma cell differentiation and chemotaxis of B cells (24) (8).

Interestingly, MSC also express matrix metalloprotease (MMP) and some members of a disintegrin and metalloprotease (ADAMs) family, both involved in cell development and migration (25). In particular, MSC release ADAMs both in exosomes and microvesicles; in this way ADAMs, released in the milieu, can cleave its ligands, such as CD30 on HL/RS membrane, preventing the recognition of an anti-CD30 antibody already used in clinical treatment (26). It should be noted that MSC also express stress molecules like NKG2DL that can be shed by ADAM10 and interfere with NKG2D during immune response (27). Taken together, this evidence indicates that MSC are involved in all tumor processes (28) (29) and they can contribute to determine an immune suppressive microenvironment also through ADAMs activity. For this reason, we focused our attention on a specific class of enzymes: ADAMs.

### Metalloproteases in cancer: the double blade of ADAMs

Metalloproteases are proteolytic enzymes defined by the presence of a  $Zn^{2+}$  ion at the catalytic site which is important in different biological processes, from cell proliferation and differentiation to physio- and pathological processes, including cancer progression. As proteolytic enzymes, they catalyse the cleavage of substrates, such as growth factors, making them available to cells; on the other hand, degradation of ECM allows cells to move through the tissues more easily. Based on the mechanism involved, we can identify two metalloprotease families: MMPs and ADAMs (30) (25). MMPs are able to degrade the ECM while ADAMs are the major proteinase family that mediates the cleavage of several substrate thanks to their proteolytic ectodomain, a process called “shedding”. In particular, ADAMs are able to shed various cell surface proteins such as growth factors, receptors and their ligands, cytokines, and cell adhesion. The proteolytic event seems to be an important step because it (i) releases an intracellular protein domain, which could act like a signal transduction molecule, and (ii) the soluble domain can act as an extracellular signal preventing the functionality of several receptors involved in the immune response.

Twenty ADAMs have been described in the human genome (31) but only 12 of these human ADAMs genes encode proteins that express the typical metalloprotease Zn-binding active site. It has been reported that ADAM9, 10 and ADAM 17 are active in several solid tumours and in haematological malignancies such as human myeloid leukaemia, myeloma, mantle cell lymphoma (MCL) and Hodgkin lymphoma (HL). ADAM10 was recently found to be one of the enzymes responsible of  $TNF\alpha$  cleavage, which is one of the activators of NF- $\kappa$ B in MCL. In addition, ADAM10 promotes cell-cycle progression and increased cell growth with the modulation of cyclin D1 and  $TNF\alpha$ /NF- $\kappa$ B signalling pathway (32). Since overexpression of

ADAM10 correlates with parameters of tumor progression, ADAMs have been proposed as both biomarkers and therapeutic targets in cancer. For this reason, ADAM10 inhibitors with anti-tumor effects have been developed. In particular, HL is characterized by an overexpression of ADAM10, and specific ADAM10 inhibitors have thus been proposed. Recently, (33) two ADAM10 specific inhibitors, LT4 and MN8, have been synthesized [11]. ADAM10 promotes an immunosuppressive microenvironment through an increased release of natural killer group-2 ligands (NKG2DL), which are involved in an impaired immune response against tumor cells in HL (34). NKG2DLs are present at low levels also in normal cells but they can be induced in stress conditions, including cancer progression. LT4 and MN8 blocked the shedding of NKG2DL in the HL cell lines L540 and L428 that, in turn, developed increased sensitivity to NKG2D mediated killing (4). All the inhibitors were also able to reduce the shedding of TNF $\alpha$ , a cytokine described as a growth factors for lymphoma cells (35).

In addition, several studies have reported the presence of ADAM10 released by HL cells and lymph node stromal cells in extracellular vehicles (EVs). Tosetti et al. reported that ADAM10 inhibitor treatment restores normal membrane CD30 levels, which rescues the sensitivity to anti-CD30 therapeutic monoclonal antibodies such as Iritumumab and Brentuximab-Vedotin, used in HL. The mechanism by which ADAM10 expression is modulated could be cell-type specific. Since ADAM10 expression is observed in both lymphocytes and stromal cells of patients, we have chosen to work with co-culture of these cells to investigate if metalloprotease inhibitors can contribute to reduce the invasive or metastatic capacity of the tumour. In particular, ADAM10 may represents key targets for selective inhibitor in novel therapeutic schemes in order to reduce immune escape of malignant cells during the course of cancer therapy.

### Therapeutic treatment for Hodgkin's lymphoma

HL is a B-cell lymphoma that affects 20-40 year old people with a second incidence peak in subjects 55 years of age and is the most common lymphoma in adolescents between 15 and 19 years of age. HL was one of first oncological pathologies to be treated by chemotherapy and radiotherapy. However, these therapies are accompanied by high toxicity and side effects; for example, the risk of coronary heart disease in HL has been shown to be related to the dose of radiotherapy. Infertility, pulmonary dysfunction and diabetes are all consequences of long-term HL treatment, beside cytopenia and immunosuppression. It is clear that this topic needs a new and viable technique to improve the lives of patients (36) (37) (38).

Based on what is known on the physio-pathology of HL, several studies have been performed on the different patterns of tumor cells; from the escape of immune response, to the cycle progression up to JAK-STAT pathway. Monoclonal antibodies (mAbs) have emerged as a major focus for drug development for a cancer treatment; however, when used alone, they do not produce long-lasting clinical benefits. For example, Nivolumab and Pembrolizumab are monoclonal antibodies that target PD-1, involved in the down-regulation of T cells in both priming phase and during the effector phase; these antibodies lead to the reactivation of T cell and T cell mediated tumor cell lysis. Interference with JAK-STAT pathway is another important aspect to be considered. Overactivation of this pathway has been linked to lymphoma, including HL. Ruvolitinib, a selective inhibitor of JAK1 e JAK2, may play useful role only in combination with other therapies. Targeting of lymphoma antigens are an alternative approach; in this contest CD30, is one of the most important candidates. CD30 is expressed on the surface of RS cells and is a member of the TNF receptor superfamily that affects cellular proliferation, survival and differentiation. CD30 is able to trigger apoptos and for this reason anti-CD30 antibodies construct with cytotoxic or radioimmunoconjugates have been developed (39). Nevertheless, these mAbs alone have not so far prove to be as effective as expected.

In 2011 the Food and Drug Administration (FDA) approved Brentuximab-Vedotin as drug for the treatment of HL. Brentuximab-Vedotin is an antibody-drug conjugate consisting of the tubulin inhibitor monomethyl auristatin E (MMAE, Vedotin) linked to an anti-CD30 mAb (Brentuximab) (40). It acts through different mechanisms: (i) delivering MMAE inside the cell after antibody internalization, where MMAE binds to tubulin preventing its polymerization, (ii) a small fraction of MMAE diffuses out of the targeted cell exerting cytotoxic effects on surrounding cells in the tumor microenvironment and (iii) since Brentuximab-Vedotin recognize CD30 antigen, the binding could induce cell-cycle arrest and apoptosis (39). Apoptosis or programmed cell death is a form of cellular death characterized by distinct phases and activation of a cascade of protease called caspases. In vitro studies have elucidated two major apoptosis pathways: (i) a stress-induced pathway mediated by cytochrome release from the mitochondria and subsequent activation of caspase 9 and (ii) death receptor-mediated pathway through the activation of caspase 8. Both pathways induce apoptosis through the activation of caspase-3. HL RS cells highly express caspase-3 and other components of the TNFR-associated signal transduction machinery like CD30 receptor. Dukers and co-workers (41) (42), using a specific antibody against the activated, cleaved form of caspase-3, found that *in vivo* B cells lymphoma apoptosis always involves the activation of caspase-3. The absence of active caspase-3 negative cells indicates that, if expressed,

apoptosis inhibitory protein such as bcl-2 and inhibitor of apoptosis (IAP) express their influence by interference with this death-signalling cascade upstream from caspase-3 activation.

However, we know that HL/RS cells are only a small fraction of the tumor mass and inflammatory cells and mesenchymal stromal cells can release chemokines that support the proliferation and survival of malignant RS cells. It seems clear how much the microenvironment is important in this contest and, based on this consideration, we planned to investigate whether ADAM10 inhibitors in combination with Brentuximab-Vedotin can improve the therapeutic effect of the antibody drug conjugate on HL/RS cells (43). We hypothesize that (i) ADAM10 inhibitors can prevent CD30 shedding and TNF $\alpha$  release from HL/RS cells, (ii) since MSC are able to release ADAM10, anti-ADAM10 will reduce the reactivity of ADAM10 release from MSC thus restoring sensitivity to the anti-CD30 Brentuximab-Vedotin; (iii) in this way Vedotin, according with the literature, can act on tubulin and induce apoptosis through caspase-3 activation (44).

#### Cell culture model: from *in vitro* 2D to 3D co-culture systems

In the field of biomedicine research, it is important to find the right model to bridge the gap between *in vitro* findings and *in vivo* study. Standard preclinical screening procedures for anticancer agents involve target identification for the compound on immortalized cell lines cultured in a 2D (two-dimensional) monolayer. Once a target has been identified experiments can be performed with *in vitro*, mainly 2D culture, or *in vivo* with animal models. Both of these strategies suffer from relevant limitations. Animal models are very expensive and require a long set up time for each tumour. Experimental data from animal tests can be limited by interspecies differences that can be difficult to overcome; this fact, in conjunction with strong ethical concerns, is a strong incentive to develop alternative models to diminish animal testing. (45) (46) (47).

2D cell monolayers have been used for a long time to predict drug effects or cell metabolism but do not resemble the complex interaction with all the other tissue cells and the cellular matrix (ECM) nor the complete tissue structure. A promising tissue engineering approach is the introduction of three-dimensional (3D) co-culture systems that can reflect cell behaviour and tissue architecture in healthy and tumour environments.

One of the first 3D co-culture systems used for *in vitro* drug screening is the spheroid model (48). A powerful improvement of tumor spheroids over conventional 2D cell cultures is the presence of metabolic and proliferative gradients across their spherical geometry that can influence pharmacological efficacy. However, they can reach the size of 500 $\mu$ m and the core may often

undergo necrosis because nutrients and oxygen are limited in the spheroid centre and there is waste accumulation. Several technologies have been developed to create spheroids with uniform size, but this model does not consider the importance of tissue architecture (49). Tissue microenvironment deeply contributes to determine both cancer progression and outcome of anti-cancer treatments; thus, newly designed *in vitro* models are being developed. Furthermore, there is increasing evidence that tumor development in humans is not fully reproducible in other animals, in particular when very complex models are designed (47). Thus, in the last years, the European Union Reference for Alternatives to Animal Testing (EURL ECVAM) has approved and validated several three-dimensional (3D) culture systems, including spheroids, as preclinical models to face and overcome these drawbacks (48). In addition, cell co-cultures that combine tumor with stromal cells in a 3D scaffold that reflect the native ECM composition can provide a biologically active microenvironment for cells to interact with (50) (45).

### Scope of thesis

To study Hodgkin lymphoma, first of all we tried to obtain a suitable system resembling the lymph node microenvironment. In this context our first aim was to obtain an *in vitro* 3D model. Starting from the spheroid co-culture system, here we propose two different approaches based on (i) decellularized lymph node matrix repopulated with lymph node derived mesenchymal stromal cells (MSC) and HL cell lines and (ii) collagen scaffolds repopulated with MSC and HL cell lines.

The second aim was to select the simplest and most reproducible model to evaluate the activity of the specific ADAM10 inhibitors LT4 and MN8 in HL, alone or in combination with Brentuximab-Vedotin, to improve its therapeutic effect. The hypothesis is that LT4 and MN8 decrease the shedding of CD30 from HL lymphocyte surface, increasing the reactivity of Brentuximab and the cytotoxic effect of Vedotin. At the same time, since ADAM10 is released in exosome and microvesicles from stromal cells using anti-ADAM10 we aim to reduce shedding from the microenvironment, decreasing the tumor immune escape.

## Materials and Methods

### Cell Cultures

To evaluate the ADAM10 inhibitor activity we used the commercially available, stabilized L428 HL cell lines, obtained from pleural effusion, and L540 cell lines obtained bone marrow of HL patients (DSMZ GmbH, Braunschweig, Germany). These cell lines, expressing both CD30 and the active form of ADAM10, were maintained in RPMI 1640 supplemented with 10% FBS, 2mM glutamine and 1% of penicillin/streptomycin (from now on we call medium B). Lymph node mesenchymal stromal cells (MSC) were cultured in  $\alpha$ -MEM (GIBCO) supplemented with 2% of Chang medium, 10% FBS (GIBCO) 2mM glutamine, 1% of penicillin/streptomycin (from now on medium A). Stabilization of MSC cultures was performed as described (34).

### ADAM10 inhibitors

Selective Adam 10 inhibitors LT4 and MN8 were synthesized and characterized as published (33). LT4 and MN8 are sulfonamido-based hydroxamate that inhibit ADAM10 by interacting with its catalytic domain and chelating the zinc ion, critical for both substrate binding and cleavage. LT4 and MN8 were used on the co-culture composed by different HL cell lines with MSC at the concentration of 10 to 20 $\mu$ M (basic on the amount of the cells used) for 48, 72 and 96 hours. 20 $\mu$ M of LT4 and MN8 were used in combination with the anti CD30 Brentuximab-Vedotin (Bre-Ved, 20 $\mu$ g/ml to 2  $\mu$ g/ml, obtained from the Pharmacy of the Ospedale Policlinico San Martino, Genoa, Italy) for the 3D collagen scaffolds experiment.

### Spheroid generation and culture

Mixed spheroids of MSC and HL cells were prepared according to the method described with some modifications (51). Briefly, 2x10<sup>4</sup> MSC were seeded in flat-bottom 96-well plates (Ultra-Low attachment multi well plates, Corning®Costar®, NY, USA) with the appropriate culture medium A, as above. On day 4, after testing MSC viability through ATP content, measured on parallel samples, and assessing that the diameter of spheroids was of about 200 $\mu$ m, 1x10<sup>5</sup> HL cells were added to the cultures, and the medium replaced with fresh complete medium B, to promote HL cell growth over MSC. After 2 days, 10 $\mu$ M LT4 or MN8 were added and the cultures were kept at 37°C, in 5% CO<sub>2</sub> humidified atmosphere for further 3 days. Generation of spheroids was monitored along time and proliferation and dimension (perimeter, area and volume) were

analyzed in each culture well 48h, 72h, or 96h after addition of LT4 or MN8. At least triplicates were analyzed for each culture condition and the number of spheroids analyzed as indicated in each figure (a minimum of 150 single spheroids for each independent experiment).

### De-cellularized matrix lymph node preparation

Lymph nodes were obtained from the Unit of Pathology, IRCSS Policlinico San Martino, Genoa, under conventional diagnostic procedures and informed consent according to the institutional ethical committee approval (IRB approval 0026910/07, renewal 03/2009, and 14/09/15). Extracellular matrix from lymph nodes was prepared following a previously described protocol (52). Some experiments were performed using as scaffolds the Avitene microfibrillar collagen sponge (3mm thick, Davol Inc., Warwick, RI).

### 3D co-cultures on LN decellularized matrix

3D cell cultures were performed by suspending  $6 \times 10^5$  MSC in 50 $\mu$ l of culture medium and seeding then onto a 50mg of fragment decellularized matrix, dipped in 1ml MSC culture medium A 1h before cell seeding. Samples were placed in a 24 well plate and kept at 37° in a 5% CO<sub>2</sub> humidified incubator for 2h, then 1ml of complete medium A was added and samples were cultured for 4 days, with medium replacement on day 2. On day 5,  $4 \times 10^5$  HL cells (either L428 or L540) were added to each ECM/MSK and cultured in medium B for further 2 days before addition of ADAM10 inhibitors. At this time, 10 $\mu$ M LT4 or MN8 were added to the culture for additional 72h or 96h. Culture supernatants (SN) were recovered after 48h to determine TNF $\alpha$  or sCD30 content and each 3D culture was embedded in paraffine for immunohistochemistry (IHC) and scanning electron microscopy (SEM).

### 3D co-cultures on collagen scaffold

First of all, we tested the capacity of MSC and L540 or L428 cells to grow inside the collagen scaffold. 24 well plates were coated with 1% sterile agarose and dried for 1 hour under hood. Sterile sheets of Avitene scaffold were cut with sterile biopsy punches (Kia Medical, Japan) into 5mm (3mm thick) fragments and then moved onto the agarose-coated plates.

MSC cells were grown in 75 T flask with medium A until sub-confluence monolayer was formed, while HL cell lines (L540 and L428) were cultured in medium B. MSC were detached from the flask with Trypsin-EDTA (Euroclone) and  $2 \times 10^5$  cells were suspended in  $30 \mu\text{l}$  of culture medium A and seeded into Avitene scaffolds. L540 and L428 were seeded at the concentration of  $4 \times 10^5$  in other scaffolds with the same procedure but in medium B. Samples were kept at  $37^\circ$  in 5%  $\text{CO}_2$  humidified incubator for 2h; then 1ml of complete medium A and medium B was added respectively to MSC and HL cells and samples were cultured for 96h, replacing medium every 2 days. Culture supernatants were recovered at different time points (24 to 96h) to analyse glucose consumption at different time.

Sequential seeding was performed by suspending  $2 \times 10^5$  MSC in  $30 \mu\text{l}$  of culture medium A and seeding on Avitene scaffold. Samples were kept for 2 hours at  $37^\circ\text{C}$  in a 5%  $\text{CO}_2$  humidified incubator, then 1 ml of complete medium A was added. Fresh cells medium was replaced after 48 hours, then the samples were further cultured for 48 hours (4 days from time 0). After 48h, HL cells (either L428 or L540) were added to the scaffold. Briefly,  $4 \times 10^5$  HL cells were suspended in  $30 \mu\text{l}$  of medium B and seeded onto the scaffold already repopulated with MSC. Samples were kept for 2 hours at  $37^\circ\text{C}$  in a 5%  $\text{CO}_2$  humidified incubator, then 1 ml of medium B was added to the scaffold and cultured for other 48 more hours.

Mixture (Mix) seeding was performed by suspending both  $2 \times 10^5$  MSC and  $4 \times 10^5$  RS cells in  $30 \mu\text{l}$  of medium A and sowing onto the scaffold. After 2h at  $37^\circ\text{C}$  in a 5%  $\text{CO}_2$  humidified incubator, medium A was added. 48 hours later medium A was replaced with medium A+ medium B (1:1), and cells grew for further 48h. In both, sequential and mix seeding conditions, culture medium was recovered after 48, 72h and 96h to determine glucose consumption at different time point.

### Images and measurement of spheroid size

Cell cultures were analyzed with Olympus IX70 bright field inverted microscope equipped with a CCD camera (ORCA-ER, C4742-80-12AG, Hamamatsu, Japan), associated to the CellSens software (version 1.12, Olympus, Tokyo, Japan). Images were taken with 10x objective NA 0.30 or 20x objective NA 0.40 (100x or 200x magnification). After calibration of the plate, a grid corresponding to each well was created and analyzed; at least five focal points were taken for each well of interest to obtain optimal images to be measured. Images of the entire well were then taken through an automated x-y axis motorized table SCAN IM 120x100-2mm (Marzhauser Wetzlar GmbH, 35579 Wetzlar, Germany). Spheroids were measured by applying the “Count and

Measure” tool of the CellSens software, after creating circular regions of interest (ROI) that represented the spheroid perimeter. Data were then transferred to GraphPad Prism software (version 5.03) for subsequent statistical analysis and data plotting. To avoid counting and measuring very small spheroids or single cells or small cell/debris aggregates, only spheroids with a diameter greater than 50µm were selected.

### Scanning Electron Microscopy of decellularized LN matrix and collagen scaffolds

Repopulated LN matrix fragments or collagen scaffolds were embedded in paraffin blocks and serially cut as 10µm thick sections using a Leica microtome. Sections were first deparaffinized using xylene and then rehydrated in decreasing concentrations of ethanol solutions. Samples slices were collected on a glass coverslip, mounted on aluminium stubs and sputter-coated for 3 minutes with gold. Morphology and ultrastructure of samples were investigated by Scanning Electron Microscopy (SEM) performed on a Hitachi TM 3000 Benchtop SEM instrument operating at 15Kv acceleration voltage.

### ATP content in spheroid co-cultures

ATP content was determined using the CellTiter-Glo® Luminescent Cell Viability Kit (Promega Italia Srl, Milan, Italy) following manufacturer’s instruction using the luciferase reaction consisting in mono-oxygenation of luciferin catalyzed by luciferase in the presence of  $Mg^{2+}$ , ATP and molecular oxygen. Luminescence was detected with the VICTORX5 multilabel plate reader (Perkin Elmer, Milan, Italy) expressed as relative light units (RLU); in some instances, the RLU were converted in µM of ATP according to a standard curve.

### Glucose Assay in co-culture medium

The amount of glucose in cells medium was evaluated through Megazyme D-Glucose Kit (K-GLUC, Megazyme). Briefly, medium from cells co-culture was collected and centrifuged in order to pellet cell debris. 10µl of medium was transferred in 96 well and 290 µl of GOPOD Reagent was added. Plate was incubated at 40°C for 20 min and absorbance was read in Victor Spectrophotometer at 510 nm for 1s.

### TNF $\alpha$ and sCD30 ELISA

Supernatants (SN) from cell cultures untreated (control condition) and treated with ADAM10 inhibitors LT4, MN8 and LT4+Bre-Ved, MN8+Bre-Ved were collected at 72 and 96 hours. CD30 shedding was measured by the specific ELISA detection kit (Human CD30 Picokine ELISA Kit from Boster Bio, TebuBio, Milan, Italy) and read at OD 450 nm. Results are expressed as pg/ml and referred to a standard curve obtained with the standard CD30 contained in the specific kit. TNF $\alpha$  was measured after treat SN for 1 hour with 1N HCl followed by 1N NaOH with a TNF $\alpha$  specific kit (PreproTech, London, UK). Results were normalized to a standard curve expressed as pg/ml.

### Hematoxylin-Eosin staining

3D co-cultures were fixed in Histochoice (Amresco, Solon, OH) overnight at 4°C. After dehydration in increasing concentrations of ethanol solutions, samples were clarified in xylene and paraffin embedded. For each scaffold 5  $\mu$ m serial sections were cut up to a depth of about 50  $\mu$ m, dried over night at 37°C. Some sections were used to performed hematoxylin eosin staining. Briefly, slides were rehydrated by decreasing concentration of ethanol solutions and coloured by hematoxylin; wash in distilled water and then coloured with eosin; finally covered with Eukitt mounting medium (Bio optica).

### Immunohistochemistry (IHC) and Immunofluorescence (IF)

For IHC and IF at least three glasses were used. In each glass three 5  $\mu$ m sections were collected and cut at a distance of 15  $\mu$ m, in order to avoid repeated analyses on the same cells.

IHC was performed after peroxy-block (Novex, Life Technologies) to quench endogenous peroxidase, followed by ultra-block reagent (Ultravision Detection System, Bio Optica, Milan, Italy). Mouse anti-human CD30 Ber-H2 (1:10, Ventana), polyclonal rabbit anti-human TGII (1:100, Thermo Scientific) and rabbit anti-human caspase-3 (1:1000, Cell Signaling) antibodies were used. Biotinylated goat anti-rabbit and anti-mouse (Biot-Gam, Bio Optica) antibodies were then added, followed by HRP-conjugated avidin (HRP-Av, Thermo Scientific) and the reaction developed using 3,3'-diaminobenzidine (DAB, Sigma) as chromogen. Slide were counterstained with hematoxylin, cover-slipped with Eukitt (Bio Optica) and analysed under Leica DM MB2 microscope equipped with Olympus DP70 with a 20x or 40x objective.

IF was performed using the automated stainer BOND RXm (Leica): slides were covered by Bond Universal Covertiles (Leica Biosystems) and placed into the Bond RXm instrument. All subsequent steps were performed according to the manufacturer's instructions (Leica Biosystem) in the following order: (1) deparaffinization with Bond Dewax Solution (Leica Biosystem) at 72°C for 30 minutes; (2) incubation with a cocktail of our two primary mouse anti-human CD30 (1:2, Ventana) and rabbit anti-human Ki67 (1:5, Ventana) at 35°C; (3) washing with Bond Wash for 4 minutes; (4) incubating with a cocktail of anti-mouse Alexa fluor-594 (1:1000) and anti-rabbit Alexa fluor-488 (1:1000) at 37°C for 30 minutes; (5) washing with Bond Wash and distilled water for 4 minutes. Slides were then counterstained with DAPI at 5µg/ml in PBS for 30 seconds and mounted with Fluoromount™ (Diagnostic Biosystem).

### Scanning and computerized imaging

IHC caspase-3 images were scanned by ApertioAT2 scanner and pictures were analysed with the Genie pattern recognition software tool (Leica Biosystems) to identify nuclei and caspase-3 positive cells. The IF staining obtained as described above, were analysed with the Aperio VERSA Digital Pathology Scanner (Leica Biosystem). Images were captured at 20x enlargement in three channels: DAPI for cell nuclei, CD30 Alexa fluor-594 for membrane stain and Ki67 Alexa fluor-488 to identify proliferating cells. Following the manufacturer's instruction, we set the score classification criteria for every class within the algorithm settings. Image data were then analysed with Aperio Cellular IF Algorithm (Leica Biosystem) that allowed to classify cells in two different classes: class 1 *KI67+* and *CD30+* cells and class 2 only *CD30+* cells, which allowed to assess the number of *CD30/Ki67+* cells (53).

## Results and Discussions

### ADAM10 inhibitors LT4 and MN8 activity on spheroid co-cultures

To test ADAM10 inhibitors on HL cells, 3D cell culture models were used: mixed spheroids of MSC and L540 or L428 were treated with 10 $\mu$ M LT4 or MN8, and cultures were kept at 37 $^{\circ}$ C for 48h, 72h or 96h.

Spheroid dimensions (fig.1, panel C) were analyzed in each cell culture as described in Materials and Methods. Of note, both LT4 and MN8 significantly reduced the size of mixed spheroids, and this effect was particularly evident after 96h. In addition, LT4 and MN8 reduced the ATP production in the spheroids in particular at 96h, while there was no effect on spheroids made by only MSC (data no shown).

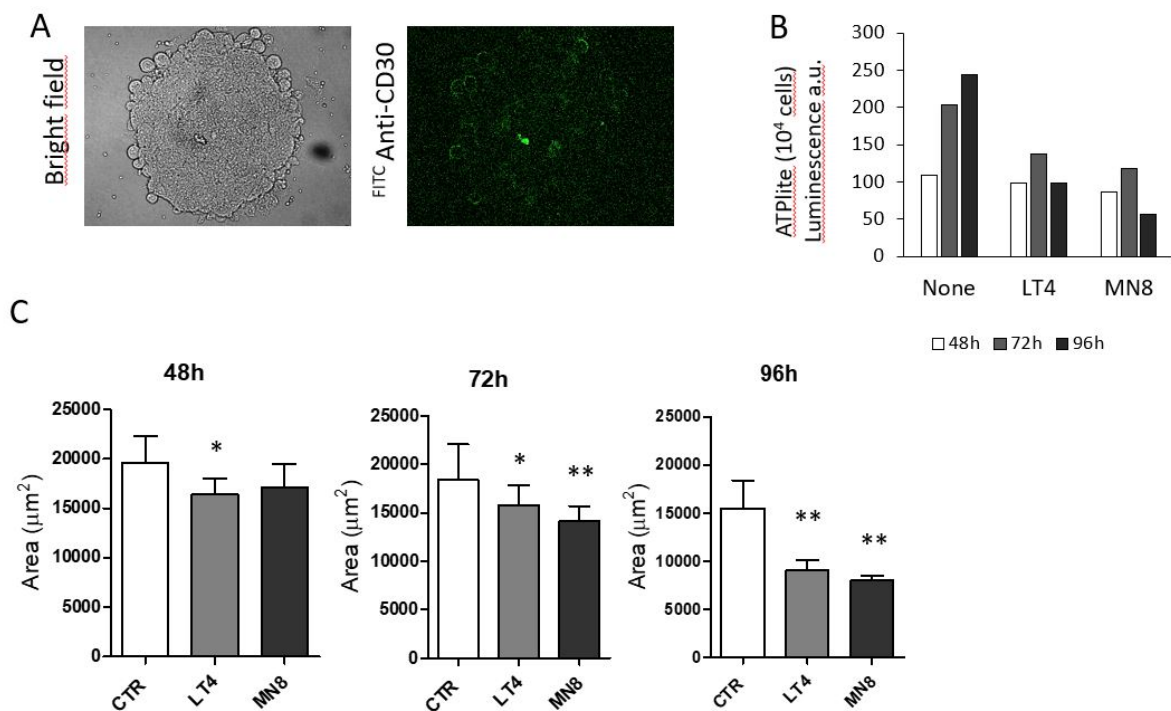


Figure 1. In A confocal microscopy of MSC and L540 mixed spheroids staining with anti-CD30; in B the ATP content in spheroids treated with LT4 and MN8 for 48, 72h and 96h was decrease compared with the control (none); in C is reported spheroids' area reduction. The spheroids size decreases especially after 96h after treatment; \* $p < 0.01$  and \*\* $p < 0.001$  vs CTR.

### ADAM10 inhibitors LT4 and MN8 reduce CD30 and TNF $\alpha$ secretion by HL cells on decellularized lymph node matrix and 3D scaffold

Matrix scaffolds from LN were seeded in 24 well plates in duplicate and repopulated with MSC ( $5 \times 10^5$ ) for 4 days and ( $4 \times 10^5$ ) L428 for further 3 days as described in Materials and Methods.

Then, 10 $\mu$ M LT4 or MN8 were added to the the cultures and 400 $\mu$ l/well were harvested at 96h for TNF $\alpha$  and sCD30 measurement by ELISA. TNF $\alpha$  has been shown to be produced by a different tumour cells, including B cell lymphomas, and acts as an autocrine growth factor while CD30 is highly express on RS cells (54). Repopulated decellularized matrices were embedded in paraffine and IHC for CD30, to identify HL cells, and TGII, to stain MSC, was performed. As visible from fig. 2, decellularized matrix was repopulated with HL cells (panel A; CD30) and MSC (panel B; TGII) and also in this 3D system, as observed in mixed spheroids, the inhibitors reduced the shedding of TNF $\alpha$  (panel C) and sCD30 (panel D), with a gradient of efficacy resultin in LT4>MN8.

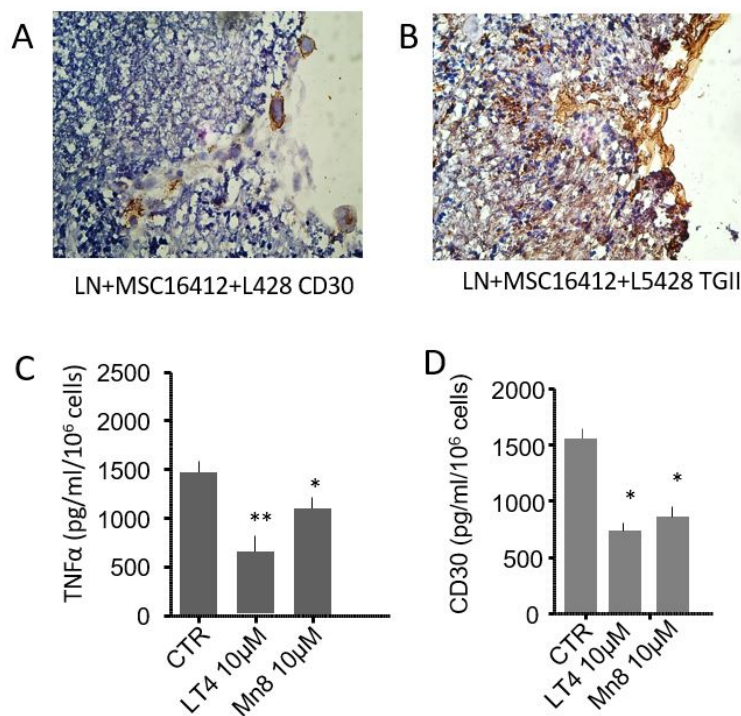


Figure 2. In A IHC for CD30 in de-cellularized matrix lymph node repopulate with MSC and L428 cells; in B IHC for TGII show MSC scaffold repopulation; in C and D ADAM10 inhibitors decrease respectively TNF $\alpha$  and CD30 secretion in 3D co-culture model made by de-cellularized lymph node with MSC and L428 cells. \*p<0.005 vs CTR; \*\* p<0.001 vs CTR.

However, decellularized matrices were difficult to obtain, were difficult to standardize, in terms of scaffold size and shape, and could barely sustain a single experiment in triplicate (i.e. three 3D replicates with MSC co-cultured with one HL cell line only). As an alternative, 3D commercially available scaffolds could represent a good choice since they correlate well to the *in vivo* situation, they were standardized and compatible with imaging techniques. In this thesis we would reproduce a lymph node using typical tissue engineering approaches through the combination of 3D co-culture and scaffold. Thus we decided to adopt commercial sponges made of microfibrillar collagen (Avitene Sponges, see Materials and Methods), already used as

hemostats in surgery. Thanks to the collaboration with Gena CNR Institute, we were able to perform a SEM characterization. Figure 3B shows the sponge, analyzed by SEM, compared to a de-cellularized LN matrix (fig.3A). The 3D structure of the sponge is similar to that of the de-cellularized matrix with a network of round shaped niches of approximately 10-50 $\mu$ M of diameter, defined by collagen fibre bundles

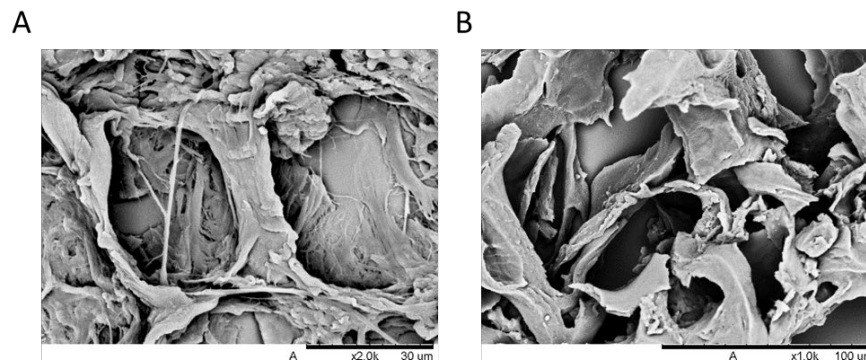


Figure 1. in A SEM of de-cellularized lymph node matrix; in B SEM of Avitene scaffold

To evaluate if the scaffold was suitable for the growth of our cells models, we first seeded MSC and L540 or L428 alone into the scaffold. Avitene sponges were cut in 5x5x3 (w x l x h) mm scaffolds;  $2 \times 10^5$  MSC or  $4 \times 10^5$  L540 (or L428) were seeded and kept in culture for 96h.

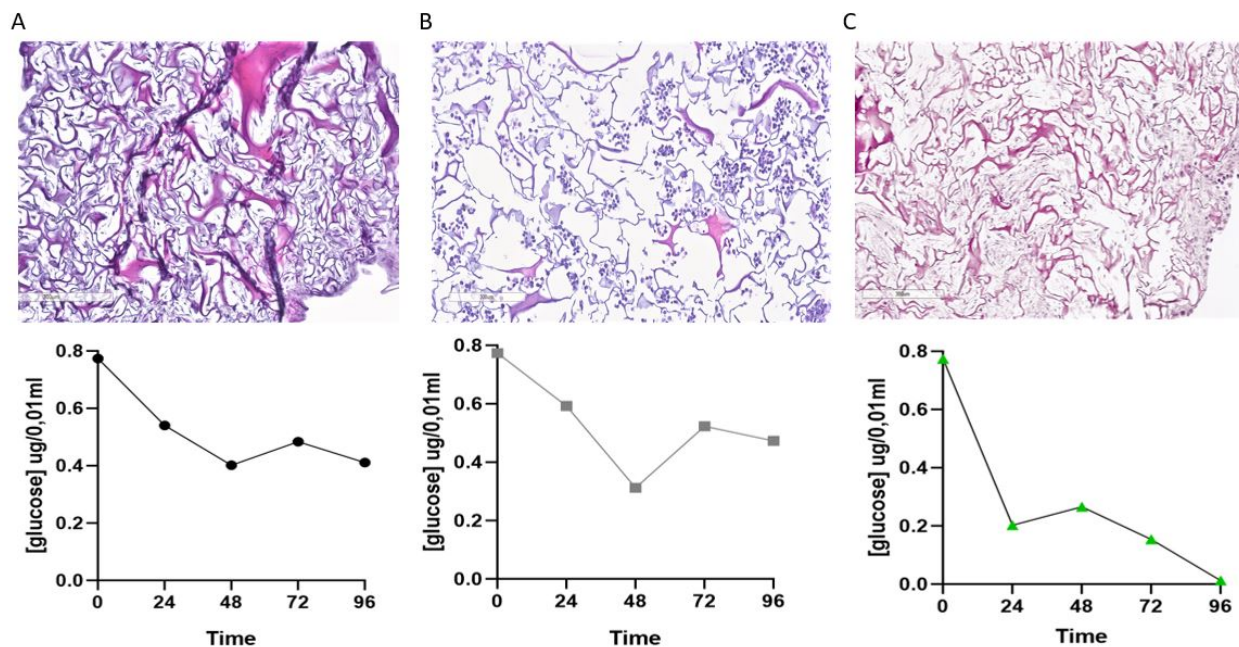


Figure 4. In A MSC on Avitene scaffold (HE staining, upper panel) and glucose concentration in the medium at the indicated time points (lower panel); B L428 on the scaffold (HE staining, upper panel) and glucose concentration (lower panel) and in C sequential seeding of MSC and L428 on the scaffold for 96h (HE, upper panel) and glucose concentration (lower Panel)

As we can see in figure 4, both MSC (panel A) and HL cells (panel B) were able to colonize the scaffold (panel A: hematoxylin-eosin staining and glucose consumption during time (lower graphs)). We can observe that scaffold architecture is much better preserved in panel A than in panel B. In fact, MSC are responsible for matrix production, which allow to preserve the scaffold architecture. L428 alone (panel B) colonized the scaffold but the internal structure was appeared much more fragmented compared with MSC (panel A). However, glucose consumption (lower graphs in panels A and B) indicates that both MSC and L428 were able to grow onto the scaffold. In order to obtain a suitable 3D *in vitro* model of HL and test ADAM10 inhibitor we proceeded with the sequential seeding as we did for the de-cellularized lymph node matrix (see materials and methods). Panel C reports the hematoxylin eosin staining: MSC and L428 were able to grow together on the scaffold while preserving the microarchitecture of the material; glucose consumption is reported in the lower graph of panel C, which shows a decrease in glucose concentration in the medium over time indicating that cells were metabolically active. Once confirmed the repopulation of the scaffolds through hematoxylin eosin staining and consumption of glucose, we proceeded to evaluate ADAM10 inhibitor activity in the culture. 20 $\mu$ M of LT4 or MN8 were added to the cultures and 400 $\mu$ l/well were harvested at 72h and 96h for TNF $\alpha$  and sCD30 measurement. As observed for spheroids and LN de-cellularized matrices, LT4 and MN8 reduced the shedding of sCD30 and TNF $\alpha$  (fig. 5) by both L428 (fig. 5A) and L540 (fig.5B) HL cells.

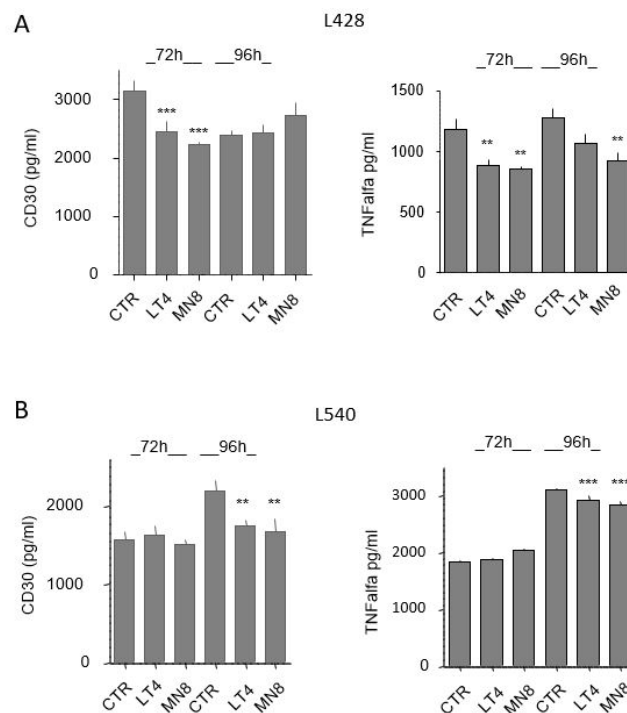
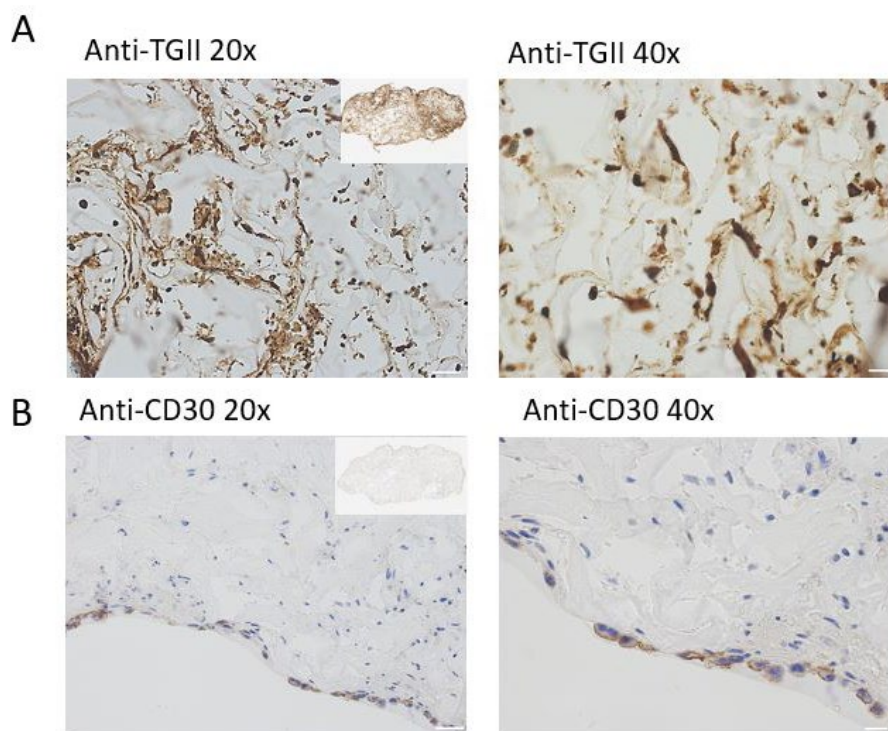


Figure 5. In A: ADAM inhibitors in MSC+L428 co-culture decrease the secretion of CD30 and TNF $\alpha$ ; in B: MSC+L540. \*\*  $p < 0.005$  vs CTR; \*\*\*  $p < 0.001$  vs CTR

The anti-sheddase effect was evident by 72h for L428 (fig. 5 panel A) and at 96h for L540 cells (fig. 5 panel B). These data suggest that the experimental model was feasible and reproducible. At the end of the culture, in order to characterize the homing of MSC and HL cells into the scaffold after 96h of culture, immunohistochemistry (IHC) was performed. IHC was performed using the automated stainer Bond RXm (Leica) in collaboration with the unit of Molecular Oncology and Angiogenesis from IRCSS Ospedale Policlinico San Martino, Genoa. To identify MSC and HL cells, the anti-TGII and the anti-CD30 antibodies were used, respectively. Scaffolds were efficiently repopulated by MSC (TGII positive, fig. 6A) and L428 cells (CD30 positive cells, fig. 6B).



*Figure 6. IHC of Avitene scaffold repopulates by sequential seeding with MSC and L428 cells. In A TGII shows MSC colonization while the insert represents the whole repopulated scaffold; in B the inset shows the negative control while the magnifiers identify CD30+ L428 cells on the scaffold*

### LT4 and MN8 inhibit HL cell proliferation in the 3D repopulated scaffolds

In a further series of experiments, we measured the effects of ADAM10 inhibitors on the proliferation of HL cells seeded in the 3D Avitene scaffold. Avitene sponges repopulated with MSC and L428 or L540 cells, as above, were exposed to 20 $\mu$ M LT4 or MN8 or in combination with Bre-Ved (20 $\mu$ g/ml) for 72h and 96h. Then, the 3D co-cultures were paraffin embedded and 5 $\mu$ m sections were prepared. IF for CD30 and Ki67, as a marker of cell cycle, was performed to

identify proliferating L540 or L428 inside the scaffold: the anti-CD30 mAb, followed by Alexafluor594-conjugated GAM, identifies RS cells (red membrane staining) and the anti-Ki67 polyclonal antibody, followed by Alexafluor488-conjugated anti-rabbit antiserum, identifies proliferating cells, while DAPI staining marks all cell nuclei (blue).

Slides were scanned with Aperio VERSA Slide Scanning and images were analyzed by ImageScope software using the Aperio Cellular IF Algorithm (Leica Biosystems). This software allows to discriminate different signals on the same cells by setting several parameters such as nucleus identification, cytoplasmic counterstain, dyes input parameters and in which cellular component they should be located in. One of the most important parameters is the scoring classification which categorizes cells in different classes. In this way the operator can create a mask that can automatically analyze the images. Our aim was to create a mask able to discriminate between  $CD30+KI67-$  (non proliferative HL cells) as class 1 and  $CD30+KI67+$  (proliferative HL cells) as class 2. According to the manufacturer's instruction and with different experiments, we set all the dyes threshold and created the macro. We analyzed at least three slides for condition using the same macro and the same parameters and calculated the amount of proliferating L540 or L428 cell over the total HL cell number in the scaffold. Figure 7 shows representative images of repopulated scaffolds, cultured for 96h captured at 20x magnification.

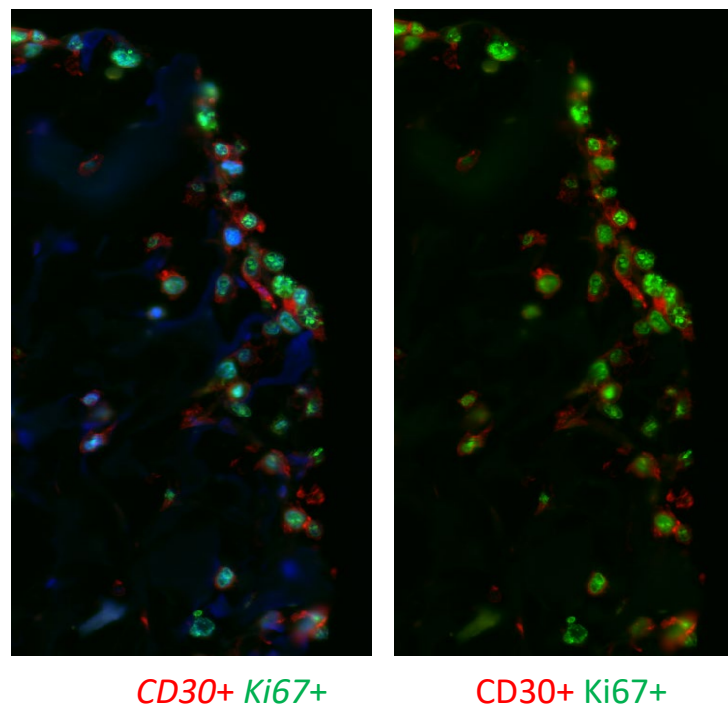


Figure 7. IF of Avitene scaffold with CD30+ HL cells (red), Ki67+ (green) as proliferating marker and nuclei (blue)

When the software analyzes the pictures, it returns a quantification, in terms of cell numbers, which can be used to quantify the cells of interest. As shown in fig 8, the number of  $CD30^+Ki67^+$  HL cells was generally lower in the presence of LT4 and MN8; the effect of LT4 was evident at 72h, while MN8 inhibition was maintained also at 96h. L540 was less sensitive to the inhibition exerted by the two ADAM10 blockers (fig.8 panel A); nevertheless, the reduction of proliferating HL cells for MN8 was significant at 96h (fig.8 right panel). We got significant results also with L428 HL cells (fig.8 panel B). The effects of ADAM10 inhibitors were evident at 72h but even at 96h were visible.

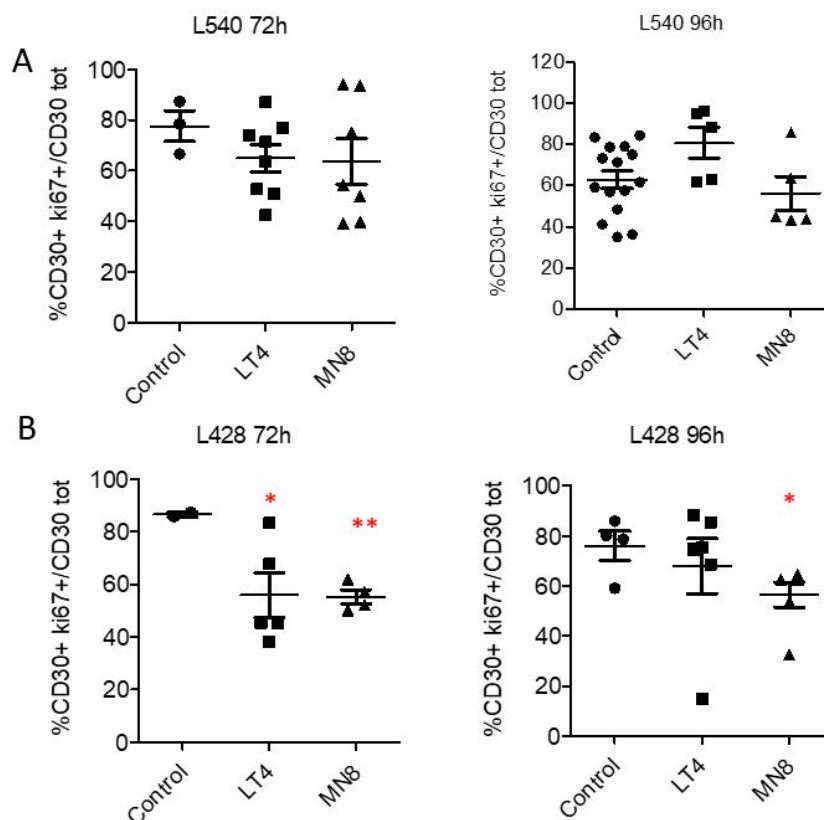
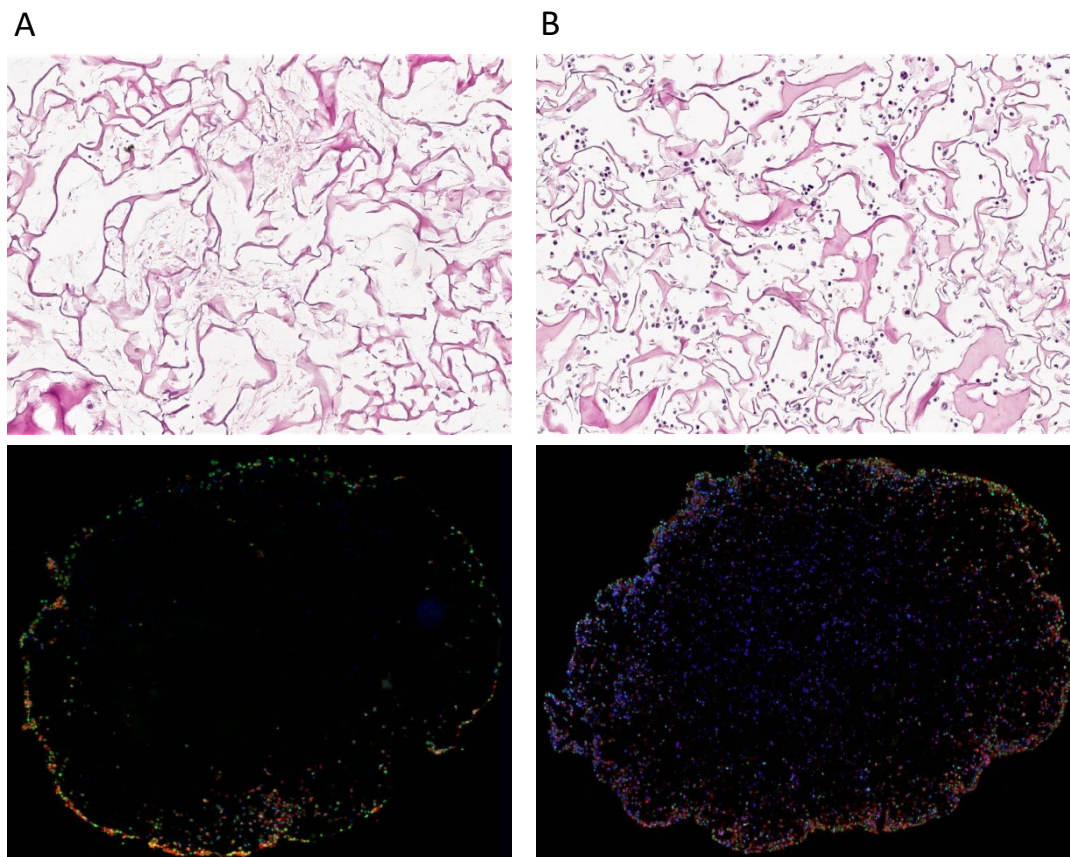


Figure 8. Quantification of  $CD30+ki67^+$ /total lymphocytes on the scaffold after ADAM10 inhibitors treatment. In A is reported the quantification about L540 cells, the effect of MN8 is visible both 72 and 96h; in B ADAM10 inhibitors effect on L428 proliferation with fewer proliferating cells at 72 and 96h after the treatment. \*  $p < 0.05$  vs control; \*\*  $p < 0.005$  vs control

### Sequential seeding and Ki67 IF do not meet our needs: mix seeding and caspase-3 IHC evaluation

Avitene scaffold represents a suitable 3D experimental model. However, with the sequential seeding the scaffolds seems to be colonized mostly in the outer portion. To better reproduce the cellularity of a LN node environment we had to improve the seeding technique. For this reason, we mixed together MSC and HL cells before seeding the mixture (mix) onto the scaffold. To

compare sequential seeding versus mixture we performed hematoxylin eosin staining and then IF for CD30- Ki67.



*Figure 9. In A upper panel HE of MSC and L428 by sequential seeding; in lower panel IF for CD30 in red, Ki67 in green and in blue nucleus; in panel B upper picture HE of MSC and L428 by mixture seeding and in the lower panel IF. With mixture seeding scaffold was repopulated also in inner areas*

The results are shown in figure 9. Comparing panel A and B, scaffolds in both conditions were repopulated and the architecture was maintained. However, as shown in the IF image of panel B, HL cells were identified not only in the outer region but also in the center of the scaffold. In contrast, as we can see in A (lower panel) with the sequential seeding HL cells were observed mainly in the outer region. Based on these findings, we chose to work with the mixture seeding that allows us a better representative repopulation.

We tried then to verify the hypothesis that the combination of ADAM10 inhibitors with Bre-Ved could increase the number of non-proliferating lymphocytes. To this aim, Ki67 turned out to be inappropriate to measure proliferating cells: indeed, since Ki67 is detectable in the nucleus not only in the mitotic phase but also in the interphase (55), Ki67 positive cells may be scored as proliferating although actually being in other cell cycle phases. For this reason, we chose to investigate apoptosis as the final effect of the combination of ADAM10 inhibitors and Bre-Ved.

Unfortunately, we could not use IF to evaluate the number of positive caspase-3 HL cells because of aspecific fluorescent signal released by the scaffold that clouded the staining with the anti-caspase-3 antibody. Thus, we analyzed caspase-3 activation in IHC as described in Materials and Methods.

### Caspase-3 activation in HL cells upon Bre-Ved and ADAM10 inhibitors treatment

In the previous paragraph we highlighted that ADAM10 inhibitors reduced CD30 and TNF $\alpha$  shedding in our experimental model. Now we focus on the apoptotic process. During the last experiment we used Brentuximab, an anti-CD30 antibody, conjugated with Vedotin, a drug that binds cytoskeletal tubulin, alone or in combination with anti-ADAM10 inhibitors. The aim was to enhance the interaction between CD30 on HL cells and Bre-Ved in order to trigger the apoptosis response. In our 3D model we tested two different concentrations of Bre-Ved (i) 20 $\mu$ g/ml and (ii) 2 $\mu$ g/ml in order to evaluate a possible synergistic effect between Bre-Ved with LT4 and MN8. We were able to detect caspase-3 positive cells on the scaffold through IHC as we can see from figure 10, panel B (treated) vs panel A(untreated). Then, the Genie software was used to calculate the amount of caspase-3 positive cells in the scaffold. In figure 10, panel C reports the percentage of positive L428 cells in all the conditions while in panel D reports L540 cells response to the treatment.

Bre-Ved at 20 $\mu$ g/ml increased the percentage of caspase-3 positive L428 cells as well as with LT4 and MN8 but a small synergistic effect was observed with Bre-Ved 20  $\mu$ g/ml+ LT4 or MN8. With regard to the concentration Bre-Ved 2 $\mu$ g/ml, we could not observe significant results in terms of increased caspase-3 positive cell.

Different results were obtained with the L540 cell line; as we can see from figure10, panel D, caspase-3 positive cells increased upon treatment with either Bre-Ved 20 $\mu$ g/ml or 2 $\mu$ g/ml. However, when Bre-Ved was used at higher concentration, no additional effect with LT4 and MN8 was been observed. Interestingly, the combination of Bre-Ved 2 $\mu$ g/ml plus LT4 and MN8 increased the percentage of caspase-3 positive L540 cells. These data suggest that further investigations are needed to elucidate the possible synergistic effect of ADAM10 inhibitors and Bre-Ved to improve the pharmacological treatment of Hodgkin Lymphoma.

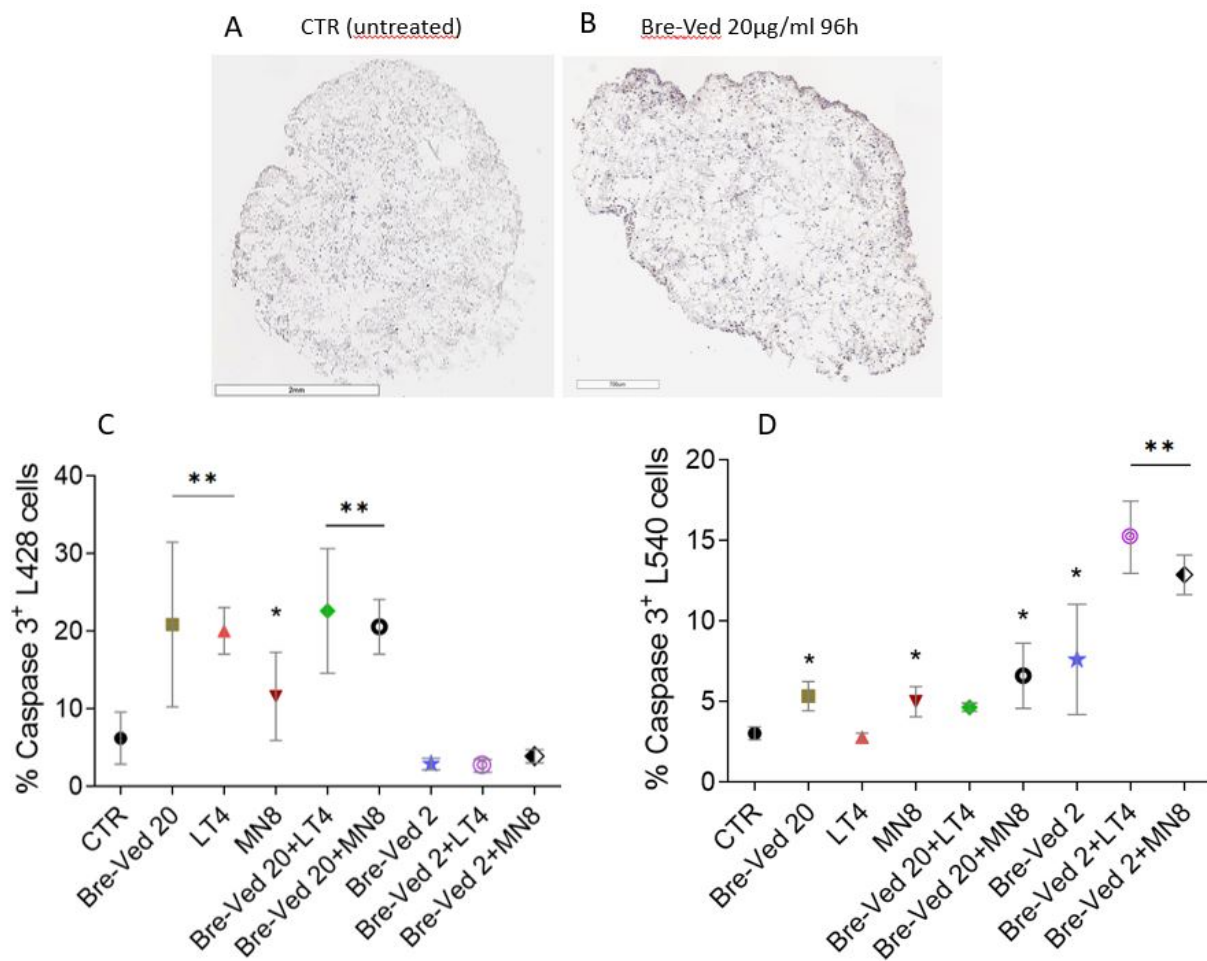


Figure 10. In A caspase-3 IHC of CTR (no treated) scaffold vs in B treated Brentuximab-Vedotin; in C quantification of positive caspase-3 cells through Genie analysis. Brentuximab-Vedotin in combination or not with ADAM10 inhibitors increase the amount of positive caspase-3 cells. C: \*\* $p < 0.0005$  and \* $p < 0.05$  vs CTR; D: \*\* $p < 0.05$  vs BtxVed and \* $p < 0.05$  vs CTR

## Conclusions

Numerous signal pathways deregulated metabolic activity in HL cells. The activation of these pathways is mediated by the interaction of HL/RS cells with other cells in their microenvironment. This microenvironment probably promotes the survival of HL/RS cells and helps them to escape immune surveillance. Considering the numerous cellular interactions, every single molecule involved may potentially offer novel strategies for targeted therapies, for instance by specific inhibition of signalling pathways. However, it is also very difficult to test new drugs since there is not a suitable published experimental model to work with. For this reason, in order to improve the therapeutic efficacy of drugs already approved for the treatment of Hodgkin's lymphoma such as Brentuximab-Vedotin, in this work we suggest different, suitable and low-cost *in vitro* 3D models of HL: mixed spheroids made of MSC and HL cells and collagen scaffold repopulated

both with MSC and HL cells; de-cellularized matrices were excluded since the experiments were not easy to reproduce. Using specific ADAM10 inhibitors, LT4 and MN8, we restored the bio-availability of CD30 in HL cells in order to increase the recognition by Brentuximab and determine the activation of apoptotic pathway through Vedotin.

In these 3D systems we found that: (i) LT4 and MN8 reduce HL cells metabolism in spheroids, i.e. ATP production related to proliferation; (ii) the two inhibitors lead to mixed spheroids size reduction and inhibition of sCD30 and TNF $\alpha$  shedding; (iii) both effects are also evident in LN matrices or collagen scaffolds repopulated with LN-MSC and HL cells.

The spheroid 3D system, approved as a pre-clinical model (51), is reproducible, cheap and allows the processing of a large number of samples. Furthermore, MSC act as a round shaped core that HL cells can use as a scaffold, and that can be easily measured in size. In this system, LT4 and MN8 could efficiently exert their anti-sheddase activity, and also interfere with HL cell metabolism, as demonstrated by ATP variations. Another consequence of the inhibitor effect is the reduction in spheroid size, conceivably due to inhibited HL cell growth. A third effect is the reduction of CD30 and TNF $\alpha$  shedding; lower amounts of TNF $\alpha$  should decrease proliferating signals delivered to lymphoma cells, while the down-regulation of CD30 shedding would maintain the expression of the molecule at the cell surface, enhancing the action of Bre-Ved. However, spheroids cannot reproduce the lymph node architecture that supports the activation of cell signaling pathways (56). For this reason, we moved to another system composed by decellularized matrix lymph node repopulate with MSC and HL cells and we tested the activity of the ADAM10 inhibitors LT4 and MN8. With this model we had results in line with the spheroid system. In particular, LT4 and MN8 were able to reduce ADAM10 sheddase activity on CD30 and TNF $\alpha$ . Of note, since the material is obtained from patients, a very long waiting time is required to reproduce the experiment. In addition, decellularized matrix were difficult to standardize in term of scaffold size and shape. Fortunately, several biomaterials can be used in order to resemble tissue architecture and optimize the 3D system. For this work we choose the microfibrillar collagen sponge Avitene, already used for hemostatic purposes in surgery. Thanks to the collaboration with the CNR of Genoa we studied our scaffold though scanning electron microscopy (SEM) and we observed that the architecture of these sponges was very similar to that of decellularized matrices obtained from lymph nodes, thus representing a good alternative to test ADAM10 inhibitors. Avitene scaffolds could be repopulated by MSC and HL cells; also in this experimental model, the anti-sheddase effect of LT4 and MN8 was documented using ELISA quantification of CD30 and TNF $\alpha$  in the supernatant at different time points and IF supporting

previous data obtained. Another aim was to study the activity of Brentuximab-Vedotin in combination with LT4 and MN8. Our hypothesis was to enhance the availability of CD30 thanks to the anti-sheddase LT4 - MN8 activity for Brentuximab and then, thanks to Vedotin activity, induce an apoptotic response in HL cells. Caspase-3 IHC shows that the percentage of caspase-3 positive cells was higher in presence of Bre-Ved. In addition, a low concentration of Bre-Ved we can improve the synergistic effect with ADAM10 inhibitors and increase its apoptotic effect on HL cells. Since the synergistic effect was not observed on both the cell lines, more studies will be performed to highlight the effects of Bre-Ved+ ADAM10 inhibitors on different cells.

In conclusion, we set up an experimental model that could represent a new promising tool to study HL in a 3D *in vitro* model reproducing the microarchitecture of the lymphoma matrix and useful for the study of pharmacological responses as well.

## Bibliography

1. *Hodgkin lymphoma*. **Ralf Küppers, 1 Andreas Engert,2 and Martin-Leo Hansmann3**. 2012, The Journal of Clinical Investigation, pp. 3439-3447.
2. *Hodgkin Disease and the Role of the Immune System*. **Alana A. Kennedy-Nasser, MD, Patrick Hanley, BS, and Catherine M. Bollard, MD**. 2011, *Pediatr Hematol Oncol*, pp. 176–186.
3. *Serum Level of the Soluble Form of the CD30 Molecule Identifies Patients With Hodgkin's Disease at High Risk of Unfavorable Outcome*. **Gianpaolo Nadali, Luisa Tavecchia, Elisabetta Zanolin, Valeria Bonfante, Simonetta Viviani, Edgarda Camerini, Pellegrino Musto, Nicola Di Renzo, Mario Carotenuto, Marco Chilosi, Mauro Krampera, and Giovanni Pizzolo**. 1998, *Blood*.
4. *ADAM10 new selective inhibitors reduce NKG2D ligand release sensitizing Hodgkin lymphoma cells to NKG2D-mediated killing*. **Maria Raffaella Zocchi, Caterina Camodeca, Elisa Nuti, Armando Rossello, Roberta Venè, Francesca Tosetti, Irene Dapino, Delfina Costa, Alessandra Musso & Alessandro Poggi**. 2016, *Oncolmmunology*.
5. *Genetic instability in Hodgkin's lymphoma*. **D. Re, T. Zander, V. Diehl & J. Wolf**. 2002, *Annals of Oncology*.
6. *Secretory pathways generating immunosuppressive NKG2D ligands*. **Aroa Baragaño Raneros, Beatriz Suarez-Álvarez and Carlos López-Larrea**. 2014, *Oncolmmunology*.
7. *How to exploit stress-related immunity against Hodgkin's lymphoma*. **Zocchi, Alessandro Poggi and Maria Raffaella**. 2013, *Oncolmmunology*.
8. *Interaction between Mesenchymal Stem Cells and B-cells*. **Linxiao Fan, Chenxia Hu, Jiajia Chen, Panpan Cen, JieWang and Lanjuan Li**. 2016, *International Journal of Molecular Sciences*.
9. *Hide or defend, the two strategies of lymphoma immune evasion: potential implications for immunotherapy*. **Houot, Marie de Charette and Roch**. 2018, *Haematologica*.
10. *Expression levels of caspase-3 in EBV positive and negative Hodgkin Lymphoma patients*. **Al-Khazaali, Ibrahim Abdul-Majeed Altamemi and Ali Sabri**. 2019, *Annals of Tropical Medicine & Public Health*.
11. *Frequent Expression of the Tumor Necrosis Factor Receptor–Associated Factor 1 in Latent Membrane Protein 1–Positive Posttransplant Lymphoproliferative Disease and HIV-Associated Lymphomas*. **PAUL G. MURRAY, PHD, LODE J. SWINNEN, MD, JOANNE R. FLAVELL, BSC, MARGARET V. RAGNI, MD, KARL R.N. BAUMFORTH, PHD, SIOBHAN M. TOOMEY, ALEXANDRA H. FILIPOVICH, MD, DEREK LOWE, PHD, CARRIE S. SCHNELL, BA, JEWEL JOHL, BA, MARGARET GULLEY, MD, LAWRENCE S. YOUNG**. s.l.: HUMAN PATHOLOGY, 2001.
12. *Serum Level of the Soluble Form of the CD30 Molecule Identifies Patients With Hodgkin's Disease at High Risk of Unfavorable Outcome*. **Gianpaolo Nadali, Luisa Tavecchia, Elisabetta Zanolin, Valeria Bonfante, Simonetta Viviani, Edgarda Camerini, Pellegrino Musto, Nicola Di Renzo, Mario Carotenuto, Marco Chilosi Mauro Krampera, and Giovanni Pizzolo**. 1998, *Blood*.
13. *Serum levels of soluble CD30 molecule (Ki-1 antigen) in Hodgkin's disease: relationship with disease activity and clinical stage*. **G Pizzolo, F Vinante, M Chilosi, F Dallenbach, O Josimovic-Alasevic, T Diamantstein, H Stein**. 1990, *British Journal of Hematology*.
14. *CD30: expression and function in health and disease*. **Watanabe, Ryouichi Horie and Toshiki**. 1998, *Immunology*.

15. *Differential effects of CD30 activation in anaplastic large cell lymphoma and Hodgkin disease cells.* **S S Mir, B W Richter, C S Duckett.** 2000, Blood.
16. *CD30 on extracellular vesicles from malignant Hodgkin cells supports damaging of CD30 ligand-expressing bystander cells with Brentuximab-Vedotin, in vitro.* **Hinrich P. Hansen, Ahmad Trad, Maria Dams, Paola Zigrino, Marcia Moss, Maximilian Tator, Gisela Schön, Patricia C Grenzi, Daniel Bachurski, Bruno Aquino, Horst Dürkop, Katrin S Reiners, Michael von Bergwelt-Baildon<sup>1</sup>, Michael Hallek.** 2016, Oncotarget.
17. *ADAM10 Inhibition of Human CD30 Shedding Increases Specificity of Targeted Immunotherapy In vitro.* **Dennis A. Eichenauer, Vijaya Lakshmi Simhadri, Elke Pogge von Strandmann, Dennis A. Eichenauer, Vijaya Lakshmi Simhadri, Elke Pogge von Strandmann, Paul Saftig, Stefan Rose-John, Andreas Engert, and Hinrich P. Hansen.** 2007, Cancer Research.
18. *Immune Checkpoint Inhibition in Classical Hodgkin Lymphoma: From Early Achievements towards New Perspectives.* **Diego De Goycoechea, Gregoire Stalder, Filipe Martins, and Michel A. Duchosal.** 2019, Journal of Oncology.
19. *Immune and Inflammatory Cells of the Tumor Microenvironment Represent Novel Therapeutic Targets in Classical Hodgkin Lymphoma.* **Eleonora Calabretta <sup>1</sup>, Francesco d'Amore <sup>2</sup> and Carmelo Carlo-Stella.** 2019, International Journal of Molecular Sciences.
20. *Mesenchymal Stromal Cells Can Regulate the Immune Response in the Tumor Microenvironment.* **Giuliani, Alessandro Poggi and Massimo.** 2014, Vaccines.
21. *Tissue transglutaminase is essential for integrin-mediated survival of bone marrow-derived mesenchymal stem cells.* **Heesang Song, Woochul Chang, Soyeon Lim, Hye-Sun Seo, Chi Young Shim, Sungha Park, Kyung-Jong Yoo, Byung-Soo Kim, Byoung-Hyun Min, Hakbae Lee, Yangsoo Jang, Namsik Chung, Ki-Chul Hwang.** 2007, Stem Cells.
22. *Transglutaminase 2 has opposing roles in the regulation of cellular functions as well as cell growth.* **H Tatsukawa, Y Furutani, K Hitomi and S Kojima and death.** 2016, Cell Death and Disease.
23. *Generation of a synthetic lymphoid tissue-like organoid in mice.* **Watanabe, Sachiko Suematsu & Takeshi.** 2004, Nature biotechnology.
24. *Human mesenchymal stem cells modulate B-cell functions .* **Anna Corcione <sup>1</sup>, Federica Benvenuto, Elisa Ferretti, Debora Giunti, Valentina Cappiello, Francesco Cazzanti, Marco Risso, Francesca Gualandi, Giovanni Luigi Mancardi, Vito Pistoia, Antonio Uccelli.** 2006, Blood.
25. *The "A Disintegrin And Metalloprotease" (ADAM) family of sheddases: Physiological and cellular functions.* **Karina Reiss, Paul Saftig.** 2008, Seminars in Cell & Developmental Biology.
26. *How to Hit Mesenchymal Stromal Cells and Make the Tumor Microenvironment immunostimulant Rather Than immunosuppressive.* **Alessandro Poggi<sup>1</sup>, Serena Varesano and Maria Raffaella Zocchi.** 2018, Frontiers of Immunity.
27. *Mesenchymal Stromal Cells Can Regulate the Immune Response in the Tumor Microenvironment.* **Giuliani, Alessandro Poggi and Massimo.** 2016, Vaccines.
28. *Bone marrow-derived mesenchymal stromal cells are attracted by multiple myeloma cell-produced chemokine CCL25 and favor myeloma cell growth in vitro and in vivo.* **Xu, S., et al.** 2012, Stem Cells.
29. *Stress immunity in lymphomas: mesenchymal cells as a target of therapy .* **Alessandro Poggi, Maria Raffaella Zocchi.** 2014, Frontiers in Bioscience.

30. *Expression of Members of the Novel Membrane Linked Metalloproteinase Family ADAM in Cells Derived from a Range of Haematological Malignancies*. **E. Wu, P. I. Croucher, and N. McKie**. 1997, BIOCHEMICAL AND BIOPHYSICAL RESEARCH COMMUNICATIONS.
31. *The evolution of ADAM gene family in eukaryotes*. **J.S.M.Souzaa, A.B.P.Lisboa, T.M.Santos, M.V.S.Andrade, V.B.S.Neves, J.Teles-Souza, H.N.R.Jesus, T.G.Bezerra, V.G.O.Falcão, R.C.Oliveira, L.E.Del-Bem**. 2020, Genomics.
32. *The many faces of metalloproteases: cell growth, invasion, angiogenesis and metastasis*. **Werb, Chieh Chang and Zena**. 2001, Trends Cell Biology.
33. *Discovery of a new selective inhibitor of A Disintegrin And Metalloprotease 10 (ADAM10) able to reduce the shedding of NKG2D ligands in Hodgkin's lymphoma cell models*. **Caterina Camodeca, Elisa Nuti, Livia Tepshi, Silvia Boero, Tiziano Tuccinardi, Enrico**. 2016, European Journal of Medicinal Chemistry.
34. *High ERp5/ADAM10 expression in lymph node microenvironment and impaired NKG2D ligands recognition in Hodgkin lymphomas*. **Maria Raffaella Zocchi, 1 Silvia Catellani, Paolo Canevali, Sara Tavella, Anna Garuti, Barbara Villaggio, Annalisa Zunino, Marco Gobbi, Giulio Fraternali-Orcioni, Annalisa Kunkl, Jean-Louis Ravetti, Silvia Boero, Alessandra Musso, and Alessandro Poggi**. 2011, Blood.
35. *TNF-alpha in onset and progression of leukemia*. **Xiaoxi Zhou, Zhuoya Li, Jianfeng Zhou**. s.l. : Experimental Hematology, 2016.
36. *Hodgkin lymphoma*. **Ralf Küppers, Andreas Engert, and Martin-Leo Hansmann**. 2012, The Journal of Clinical Investigation.
37. *Hodgkin's disease: a tumor with disturbed immunological pathways*. **Hans-Jiirgen Grur, Antonio Pinto, Justus Duyster, Sibrand Poppema and Friedhelm Hermann**. 1997, Immunology today.
38. *Hodgkin's Lymphoma Therapy: Past, Present, and Future*. **Rathore, M Kadin and B**. 2010, NIH Public Access, pp. 2891–2906.
39. *Treatment of Hodgkin Lymphoma – New and Developing Therapies and Their Potential Role in Standard of Care*. **Böll, Theodoros P Vassilakopoulos and Boris**. 2019, European Oncology and Haematology.
40. *Brentuximab Vedotin (SGN-35)*. **Jessica Katz, John E. Janik, and Anas Younes**. 2011, Clinic Cancer Research.
41. *High numbers of active caspase 3–positive Reed-Sternberg cells in pretreatment biopsy specimens of patients with Hodgkin disease predict favorable clinical outcome*. **Danny F. Dukers, Chris J. L. M. Meijer, Rosita L. ten Berge, Wim Vos, Gert J. Ossenkoppele, and Joost J. Oudejans**. 2016, Blood.
42. *clAP2 is highly expressed in Hodgkin–Reed–Sternberg cells and inhibits apoptosis by interfering with constitutively active caspase-3*. **Horst Dürkop, Burkhard Hirsch**. 2006, Molecular Medicine.
43. *Targeting ADAM10 in Cancer and Autoimmunity*. **Timothy M. Smith Jr., Anuj Tharakan and Rebecca K. Martin**. 2020, Frontiers in Immunology.
44. *High numbers of active caspase 3–positive Reed-Sternberg cells in pretreatment biopsy specimens of patients with Hodgkin disease predict favorable biopsy specimens of patients with Hodgkin disease predict favorable biopsy specimens of patients with Hodgki*. **Danny F. Dukers, Chris J. L. M. Meijer, Rosita L. ten Berge, Wim Vos, Gert J. Ossenkoppele, and Joost J. Oudejans**.

45. **Williams, S. J. Enna and M.** Defining the Role of Pharmacology in the Emerging World of Translational Research. *Pharmacology and Translational Research*. 2009.
46. *Experimental Models as Refined Translational Tools for Breast Cancer Research*. **Eduardo Costa, Tânia Ferreira-Gonçalves, Gonçalo Chasqueira, António S. Cabrita, Isabel V. Figueiredo, and Catarina Pinto Reis**. 2020, Scientia Pharmaceutica.
47. *The flaws and human harms of animal experimentation*. **A., Akhtar**. 2015, Camb and Health Ethics.
48. *Emerging tumor spheroids technologies for 3D in vitro cancer modeling*. **26. Rodrigues T, Kundu B, Silva-Correia J, Kundu SC, Oliveira JM, Reis RL, Correlo VM**. 2017, Pharmacol Ther.
49. **Elizaveta V. Koudan, 1 Janetta V. Korneva,2 Pavel A. Karalkin,1 Irina S. Gladkaya,1 Anna A. Gryadunova,1 Vladimir A. Mironov,1 Yusef D. Khesuani,1 and Elena A. Bulanova**. The Scalable Standardized Biofabrication of Tissue Spheroids from Different Cell Types Using Nonadhesive Technology. *3D PRINTING AND ADDITIVE MANUFACTURING*. 2017.
50. *Application of tissue engineering to the immune system: development of artificial lymph node*. **TomCupedo, AbrahamStroock and MarkColes**. 2012, Frontiers in Immunology.
51. *Spheroid-based drug screen: considerations and practical approach*. **Juergen Friedrich, Claudia Seidel, Reinhard Ebner & Leoni A Kunz-Schughart**. 2009, Nature Protocols.
52. *Insight On Colorectal Carcinoma Infiltration by Studying Perilesional Extracellular Matrix*. **Manuela Nebuloni, Luca Albarello, Annapaola Andolfo, Cinzia Magagnotti, Luca Genovese, Irene Locatelli, Giovanni Tonon, Erika Longhi, Pietro Zerbi, Raffaele Allevi, Alessandro Podestà, Luca Puricelli, Paolo Milani, Armando Soldarini, Andrea Salonia & Massimo Alfano**. 2016, Scientifica Reports.
53. *Calcitonin Receptor-Like Receptor and Receptor Activity Modifying Protein 1 in the rat dorsal horn: localization in glutamatergic presynaptic terminals containing opioids and adrenergic  $\alpha 2C$  receptors*. **Juan Carlos G. Marvizón, Orlando A. Pérez, Bingbing Song, Wenling Chen, Nigel W. Bunnett, Eileen F. Grady, and Andrew J. Todd**. 2007, Neuroscience.
54. *CD30: expression and function in health and disease*. **Watanabe, Ryouichi Horie and Toshiki**. 1998, Immunology.
55. *Ki-67: more than a proliferation marker*. **Kaufman, Xiaoming Sun and Paul D**. 2018, Chromosoma.
56. *Framing cancer progression: influence of the organ- and tumour-specific matrix*. **Erler, Maria Rafeeva and Janine T**. FEBS Journal 2019.
57. *Linearized texture of three-dimensional extracellular matrix is mandatory for bladder cancer cell invasion*. **Massimo Alfano, Manuela Nebuloni, Raffaele Allevi, Pietro Zerbi, Erika Longhi, Roberta Lucianò, Irene Locatelli, Angela Pecoraro, Marco Indrieri, Chantal Speziali, Claudio Doglioni, Paolo Milani, Francesco Montorsi & Andrea Salonia**. 2016, Nature.